Journal of Materials Chemistry B

Accepted Manuscript

ROYAL SOCIETY OF CHEMISTRY

www.rsc.org/materialsB

Synthesis and Crystal Structure of one novel Copper(II) Complex of Curcumin-type and Application for *in vitro* and *in vivo* Imaging

Guoyong Xu [a]，Jiafeng Wang [b]，Tao Liu [b] , Mahong Wang [a],
Shuangsheng Zhou [*abc]， Baoxing Wu[bc], Minghua Jiang [c]

[a] *Center of Modern Experimental Technology, Anhui University, Hefei 230039, P. R.China*

[b] *Department of Pharmacy, Anhui University of Chinese Medicine, Hefei 230038, P.R .China*

[c] *State Key Laboratory of Crystal Materials, Shandong University, Jinan 502100, PR China*

ABSTRCT: A novel multibranch Cu(II) complex $\mathbf{CuL_2 \cdot C_4H_8O_2}$(L = 1,7-bis(4-ethyloxy-3-methyloxy-phenyl)-1,6-heptadiene-3,5-dione) was obtained and the crystal structure was determined. The linear photophysical properties, two-photon absorption (2PA), and photostability behavior of the obtained complex were investigated. The experimental results show the complex exhibits larger 2PA cross section in the NIR region, higher quantum yield and photostability and lower cytotoxicity. The *in vitro* study utilized the human breast cancer MCF-7 cell line that was imaged by two-photon fluorescence microscopy. The tumor targeting capability of the complex on tumor–bearing nude mice *in vivo* demonstrated its high targeting capability to test cancerous cells. These results suggest that the Cu(II) complex is a probe for *vivo* promising.

Keywords: copper(II) complex of curcumin-type; crystal structure; NIR probe; cell imaging; early tumor imaging

1. Introduction

Material molecules with large two-photon absorption (2PA) cross sections have attracted increasing attention due to their versatile applications in optical power limiting, 3-D data storage, bio-imaging and tracking, photodynamic therapy.[1] Among them, bioimaging as one of the most practical methods in living cells and tissues has given rise to great interest, which can detect biological activity in vivo, assess disease-related molecular expression for earlier detection of disease and evaluation of drug effects in clinical applications, as well as monitor the dynamic behavior of chemical components of tissues, understands the metabolism, structure, signal transduction and transmission.[2] For earlier detection of disease, up to now, several imaging modalities have been used for investigation of disease. For example, computed tomography (CT) may use for tumor staging, but offers poor soft tissue contrast with resulting poor sensitivity and specificity in screening.[3] Magnetic resonance imaging (MRI) offers many incline surface imaging without ionizing radiation, but it is too expensive to high throughput screening.[3(a)] Positron emission tomography (PET) with a very high sensitivity can interrogate various molecular/biochemical properties, but is more suitable for monitoring response to therapy than detecting early lesions due to limited spatial resolution. [3(a), 4] In addition, traditional fluorescence imaging using ultraviolet and visible light has many disadvantages, such as poor tissue penetration, a low signal-to-noise ratio and the images are not clear.[5] In contrast, Two-photon microscopy (2PM) offers many advantages over current imaging techniques, such as increased penetration depth,

lower autofluorescence and self-absorption, clear imaging, prolonged observation time and detecting early diagnosis of tumor [6]. El-Sayed's group [7] has prepared anti-EGFR antibodies conjugated gold nanoparticles, which are found to distinguish between cancerous and noncancerous cells. Gu et al. [8] have studied demonstrated that the as-prepared compound resulted in high targeting capability to FR over-expressed tumor, it can be used as efficient probes to imaging tumor *in vitro* and *in vivo*. Hayashi and co-workers [9] have developed a near-infrared (NIR) fluorescent silica–porphyrin hybrid nanotubes (HNTs), the fluorescence of the HNTs-labeled macrophages was clearly detected *in vivo*, and even the minimum detectable number of cells was 200. Furthermore, Li's group [10] found that the collagen distributions in the nomal thyroid tissue and nodular thyroid tissue are different by using two-photon excited fluorescence (2PEF) and second harmonics generation (SHG) techniques . These results suggest the TPM imaging can distinguish between nomal thyroid tissue, nodular thyroid tissue and papillary thyroid carcinoma tissue, and use for rapid diagnosis of thyroid cancer.

However, for cell imaging applications, it is necessary that the two-photon absorption (2PA) materials are highly fluorescent in high polar media. A great many 2PA materials, however, caused the fluorescent quenching in polar solvents own to the poor photostability and the aggregation of molecules.[11] Accordingly, 2PA materials for cell imaging should be designed to ensure large two-photon activity, low toxicity and good photostability, but more importantly to overcome fluorescence quenching in strong polar media. By combining experiments and theoretic calculation,

Marder [12] and Perry [13] found that molecules with donor-acceptor-donor(D-A-D), acceptor-donor-acceptor(A-D-A), multipolar structural motifs possess good optical properties, furthermore the increase of the donor strength and the conjugation length will lead to an increase in the 2PA cross section. However, the synthesis of multipolar molecules bearing π-conjugated motifs incorporating donor and acceptor moieties requires extraordinary synthetic skills and generally gains very low-yielding of the desired products, and thus are less favorable for large-scale production.

Curcumin is a natural pigment with low toxicity and good stability, which is obtained from the rhizomes of turmeric (Curcuma longa Linn.) and often used in spices, cosmetics and traditional chinese medicine in Asian country. In addition, curcumin shows good optical and electrical properties owing to symmetric structure containing β-diketone and large π-conjugation length in polar media.[14] Based on the above strategy and our previous work.[15] In this work, we firstly connect two electron-donating ethyl groups to 4, 4′-diphenolic hydroxyl group positions of the curcumin to get one bipolar-type D-A-D curcumin derivative [1,7-bis(4-ethyloxy-3-methyloxy-phenyl)-1,6-heptadiene-3,5-dione, labeled as **HL** in Fig. 1a] and then form quadrupolar-type Cu(II) complex (labeled as $\mathbf{CuL_2 \cdot C_4H_8O_2}$) by reaction with copper acetate. It is predicted that the multielectron-donating complex should have excellent one-/two-photon fluorescence properties and 2PA cross section. Furthermore, application of the obtained complex as near-infrared (NIR) fluorescent probes for the imaging of cancer cells *in vitro* and *in vivo* were also investigated.

2. Materials and methods

2.1 Materials and general instruments

All chemicals were available commercially and every solvent was purified as conventional methods before use.

Elemental analyses were performed on Perkin-Elmer 240C analyzer. the elemental analysis data of metal copper is obtained by ICAP Q ICP-MS(Thermo Scientific, Germany). Fourier transform infrared(FT-IR) spectra were recorded on SHIMADZU IR Prestige-21 spectrophotometer with samples prepared as KBr pellets. The mass spectra were obtained on FINNIGAN LCQ Advantage MAX LC/MS (Thermo Finnigan, American). Single-crystal X-ray diffraction measurements were carried out on a Seimens Smart 1000 CCD diffractometer equipped with a graphite crystal monochromator situated in the incident beam for data collection at room temperature. The determination of unit cell parameters and data collections were performed with Mo Ka radiation (λ = 0.71073Å) (shown in Table S1). Unit cell dimensions were obtained with least-square refinements, and all structures were solved by the direct method as SHELXL-97.[16] The final refinement was performed by full-matrix least-square methods with anisotropic thermal parameters for non-hydrogen atoms on F^2. The linear absorption spectra were measured on a UV-3600 spectrophotometer. The one-photon excited fluorescence(1PEF) spectra measurements were performed using an F-7000 fluorescence spectrophotometer (Japan).

2.2 Synthesis

2.2.1 Synthesis of 1,7-bis(4-butyloxy-3-methyloxy-phenyl)-1,6-heptadiene-3,5-dione (**HL**) [17a]

Dimethylfomamide (20 mL) and curcumin (1.0 g, 2.7 mmol) were placed into a 50 mL flask. After the curcumin was completely dissolved, anhydrous potassium carbonate(1.2 g, 0.87 mmol) was added. The mixture was stirred at 40 □, and then bromoethane (2.0 mL) was slowly added dropwise to the above solution. Then the reaction mixture was stirred for 5 h at 80□. After completion of the reaction (monitored by TLC), the mixture was dispersed and stirred into cold water (50 mL). The yellow solid was obtained by filtration. The product was purified by chromatography on a silica gel column with ethyl acetate/petroleum ether mixture (v/v: 2/3) as the eluent, then light yellow microcrystals were obtained, yield 65.4%. MS, m/z (%): 424.47(M^+, 100). Anal. Calcd for $C_{25}H_{28}O_6$: C, 70.74; H, 6.65; found: C, 70.53; H, 6.84.

2.2.2 Preparation of the Cu(II) complex (**$CuL_2 \cdot C_4H_8O_2$**)

$Cu(OAc)_2 \cdot 3H_2O$ (0.13 mmol) and HL(0.06 mmol) were dissolved in 5 mL of ethyl acetate. The solution was stirred at room temperature until a lot of precipitation formed and hen filtered. The crude product was washed by dichloromethane (15 mL × 3), CH_3CN (15 mL × 3) and EtOH(15 mL × 3), respectively. yield 67.3%. IR (KBr), ν(cm^{-1}) ： 2979, 1625, 1510, 1598,1577, 1477 (Ar)，1252, 541； Anal. Calcd for $C_{54}H_{62}CuO_{14}$: C, 64.99; H, 6.21; Cu, 6.37; found: C, 64.64; H, 6.13; Cu, 6.18.

2.3 Cell Viability Tests

Human MCF-7(breast cancer) cells were seeded into a 96-well culture plate at 2.0 × 10^4 cell/well. Then 50 μL of CuL_2 diluted with DMEM at different concentrations was added to each well, respectively. The cells were incubated for 24 h at 37 °C and

5% CO_2, followed by the addition of 40 μL MTT solution(5 mg/mL) to each well and incubated for an additional 4 h (37 °C, 5% CO_2).Then, DMEM was removed, the cells were dissolved in DMSO (150 μL/well), the absorbance of each cell was measured by UV spectrometer at 570 nm. The percentage of viable cells was calculated relative to untreated cells.

2.4 Cell Culture and Staining

MCF-7 cells were passed and plated on a 35-mm cell culture dish with a coverslip and cultured in Dulbecco's Modified Eagle Medium (DMEM) (Gibco) supplemented with 10% fetal bovine serum (Sigma), penicillin (100 μg mL^{-1}), and streptomycin (100 ug mL^{-1}) at 37 °C in a humidified atmosphere with 5% CO_2 and 95% air for 24 h prior to staining. Immediately before labeling, cells were washed with PBS (phosphate buffered saline, pH =7.1, Gibco) 3 times to remove the growth medium, and then 10 μL of the CuL_2 complex in DMSO(0.2 mM) and 190 μL of PBS were added into the dish. After 30 min of incubation at 37 °C, 5% CO_2, the cells were washed with PBS to remove unlabeled molecules, and then the cells were taken to a two-photon microscope for imaging.

2.5 Animal Experiments and *In vivo* Cell Imaging

Normal Kunming mice were purchased from Laboratory Animals of China Pharmaceutical University.(Nanjing, China). All animal experiments were carried out in compliance with the Animal Management Rules of the Ministry of Health of the People's Republic of China. Tumor-bearing mice were prepared by following the previously described method.[18] Briefly, 20 Kunming nude mice (weighed 35 ~ 40 g,

equal number of male and female subjects) were divided into 2 groups. One group was experiment groups (n = 10, 5 males and 5 females in each group), another group was used as normal control groups (n = 10, 5 males and 5 females in each group). Then Bel-7402 tumor cells (2~ 4 × 10^5 cells per mouse) was implanted on the left axilla of experiment group nude mice. At about fifteen days after transplantation, the tumor grew up to a diameter of reached about 0.1~ 0.2 cm, then, the mice were selected under anaesthetic for *in vivo* optical imaging, including the normal control group (3 males and 3 females in each group) and Bel-7402 tumor-bearing mice group (3 males and 3 females in each group). The Cu(II) complex probe (20 μM, 0.2 mL) was administered into each tumor-bearing and normal mouse through tail vein injection. Forty minutes after injection of the probe, fluorescence imaging was acquired using the IVIS Lumina system (Xenogen Co., Alameda, CA, USA).

3. Results and discussion

3.1 Structural features

The structures of **HL** and $\mathbf{CuL_2 \cdot C_4H_8O_2}$ were further confirmed by single-crystal X-ray diffraction. Single crystal of the obtained complex suitable for X-ray crystallography analysis was grown from ethyl acetate/1,4-dioxane (Fig. 1b). Compound **HL** crystallizes in the monoclinic space group P2(1)/n. This kind of structure has been described by us before.[17a] As shown in Fig. 1b, each copper(II) center has a square planar coordinated sphere surrounded by four oxygen atoms from two β-diketonato fragments. As shown in Table S1 (Supporting Information), the Cu1-O3 and Cu1-O4 bond lengths are 1.9031(18) and 1.9282(18), respectively, which

are smaller than those in other copper diketonate complexes.[19] Two β-diketonate ligands oriented at the equatorial positions in the quadrupolar-type copper(II) complex are almost coplanar with the torsion dihedral angle from 172° to 175°. In addition, the bond lengths are intermediate, such as C5-C7 [1.465(3) Å], C7-C8 [1.337(4) Å], C8-C9 [1.474(3) Å], C9-C10 [1.402(4) Å], C10-C11 [1.410(3) Å], C11-C12 [1.474(3) Å], C12-C13 [1.337(3) Å] and C13-C14 [1.468(3) Å]. The structural character of the complex indicates there is a almost coplane and large π-conjugated system, which is a necessary for large 2PA cross-section. The packing diagram of the complex (Fig. 1c) shows that the adjacent molecules are stacked through two types of π–π interactions along the a and c axises with the short distance of 3.846 and 3.897 Å, respectively (more information shown in Supporting Information, Fig. S3)

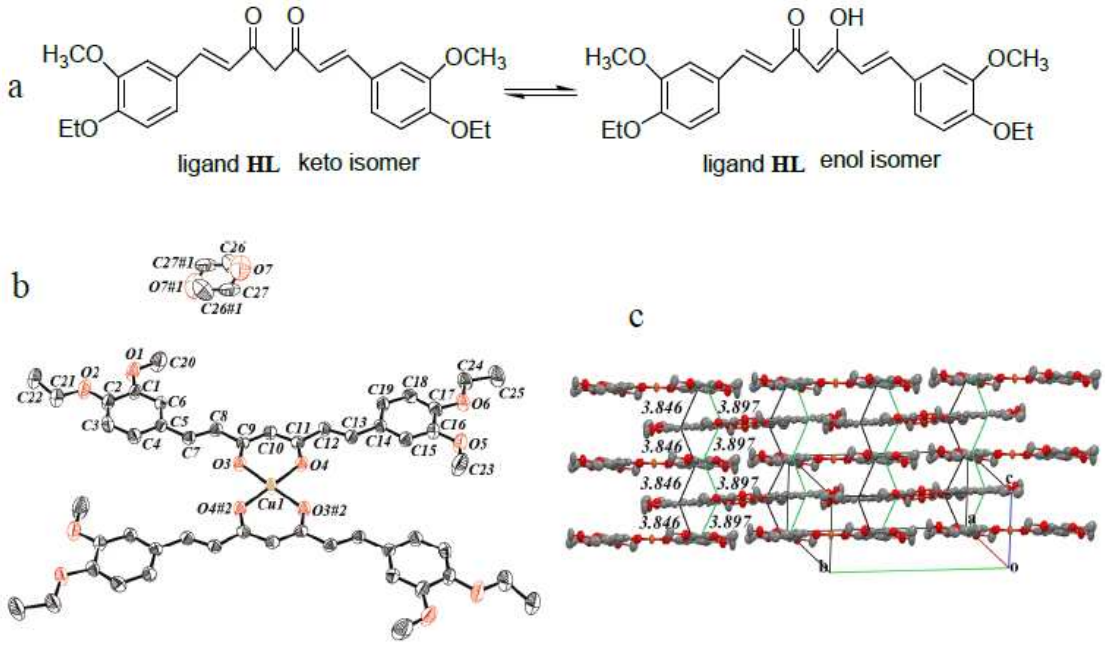

Fig. 1 (a) Molecular structure of **HL**. (b) ORTEP structure of $\mathbf{CuL_2 \cdot C_4H_8O_2}$ with 50% probability(all hydrogen atoms are omitted for clarity). (c) The packing diagram of the Cu(II) complex.

3.2 Linear absorption and one-photon excited fluorescence(1PEF) of the compounds

The linear absorption spectra of the compounds **HL** and its Cu(II) complex in DMF (c = 10 μM) were shown in Fig. 2a. It is clearly exhibited that the absorption behaviors of the two compounds are almost the same because of their similar structures. The wavelengths of two peaks are 265 and 384 nm for **HL**, 267 and 387 nm for the complex. The longer-wavelength peak in each compound is attributed to the π→π* absorption of larger π-conjugated main chain (log ε = 3.5 – 4.0),[20] and the second peak is attributed to the n→π* absorption associated with p–π conjugation between oxygen lone-pair electrons and benzene. Moreover, the obtained complex showed relatively stronger absorbance than the pure ligand, this can be easily understood because the complex compound contains two ligand molecules. Fig. 2b shows one-photon excited fluorescence (1PEF) spectra of the two compounds in DMF solution (c = 10 μM), and the maximum emission wavelengths both locate at about 520 nm. Their 1PEF spectra are also similar due to structural comparability and show the same sensitivity to the polarity of solvent molecules. The linear absorption and 1PEF spectra of the two compound in several solvents with different polarity exhibit significant solvatochromic phenomenon (Table 1，Figures S4 and S5). The positive solvatochromism illustrates a larger stabilization of the excited state than the ground state in a polar solvent. It implies that a significant charge redistribution takes place upon excitation, which is in conformity with multidimensional intramolecular charge transfer (MDICT). [21]

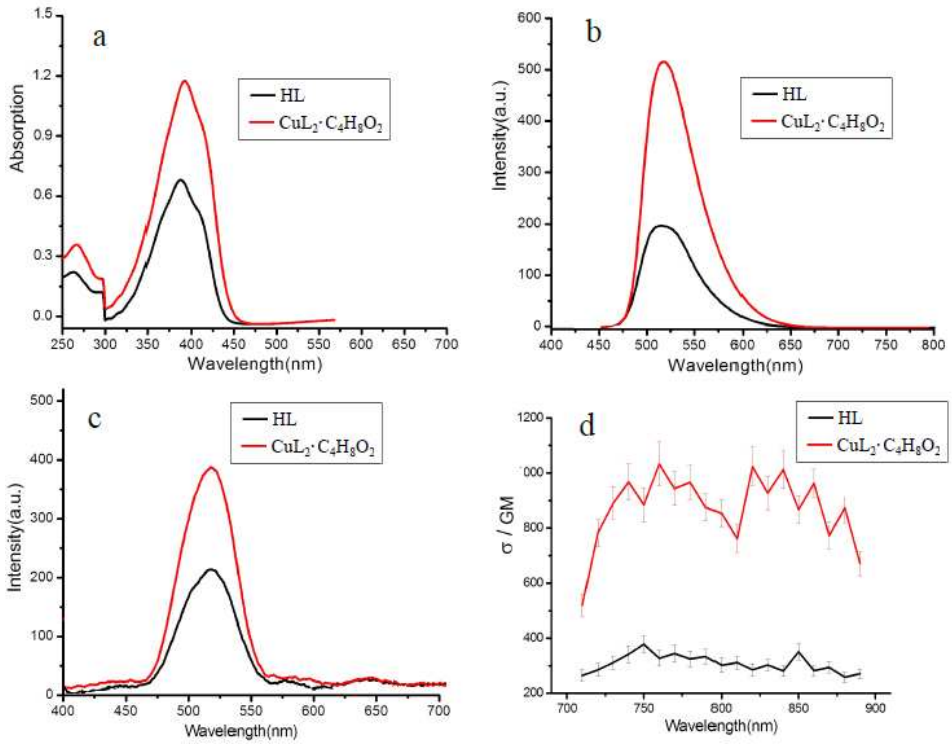

Fig. 2 Linear absorption(a), 1PEF(b) and 2PEF(c) spectra of the two compounds in DMF. (d) 2PA cross-section of the compounds in DMF versus excitation wavelengths of identical energy of 0.380 W.

To further demonstrate the influence of solvent on fluorescence, Table 1 lists the Stokes shift of the two compounds in different polar solvents. The Stokes shift is defined as the loss of energy between absorption and emission of light, which is a result of several dynamic processes. These processes include losses arising from the dissipation of vibrational energy, redistribution of electrons in the surrounding solvent molecules induced by the altered dipole moment of the excited chromophore, reorientation of the solvent molecules around the excited state dipole, and specific interactions between the chromophore molecular and the solvent or solution molecular. The Lippert equation [Eq. 1] is widely used to describe the effects of the photophysical properties of the solvent on the emission spectra of a chromophore.[22]

$$\Delta\nu = \nu_{abs} - \nu_{em} = (2/cha^3)\,\Delta f(u_e - u_g)^2 + \text{const.} \quad (1)$$

Where c is the speed of light, h is Planck′s constant, and a is the radius of the cavity in which the chromophore resides. ν_{abs} and ν_{em} (in cm^{-1}) are the wavenumbers of the absorption and emission, respectively. In aprotic solvents, Stokes shifts are approximately proportional to the orientational polarizability.[23]

Table 1 The photophysical properties of HL and CuL_2 in different solvents

Comd.	Solvent	Λ_{max}^{abs} / nm	$\varepsilon/10^4$	λ_{max}^{1f} /nm	λ_{max}^{2f} /nm	Φ [a]	$\Delta\nu$ [b]	σ_{max} [c]
HL	CH_2Cl_2	371	4.13	491		0.18	6583	425
	EtOH	380	3.82	499		0.31	6280	417
	DMF	384	3.64	512	520	0.43	6719	374
	DMSO	381	3.42	520		0.54	7009	391
CuL_2	CH_2Cl_2	386	4.36	493		0.22	5626	1128
	EtOH	391	4.13	500		0.37	5570	1051
	DMF	387	3.92	512	521	0.48	6309	1036
	DMSO	404	3.77	520		0.64	6519	1042

λ_{max}^{abs} and λ_{max}^{1f} represent the maximum wavelength of linear absorption and single-photon fluorescence, respectively. It is filtered through a 0.2 mm Gelman acrodisc CR filter.

[a] quantum yield (Φ) at room temperature was determined with Coumarin($\Phi r = 0.56$ in ethanol) as a reference in DMF.

[b] Stokes shift in cm^{-1}. [c] two-photon absorption cross-section in GM (1GM= 10^{-50} cm^4 s $photon^{-1}$ $molecule^{-1}$).

3.3 Two-photon absorption propert (2PA) and 2PA cross section

Fig. 2c shows the two-photon excited fluorescence(2PEF) spectra of two compounds in DMF with a concentration of c = 10 μM. The 2PEF measurement was taken with a certain laser beam from a mode-locked Ti:sapphire laser (Coherent Mira 900 F) as the pump source with a pulse duration of 200 fs. The excitation wavelengths of HL and its Cu(II) complex are 820 and 840 nm, respectively. From Fig. 2b and Fig. 2c, it was found that the 2PEF spectra of the two compounds in DMF are essentially

the same as their 1PEF spectra, confirming that both emissions are from the same excited state.

The compounds HL and Cu(II) complex of the photoluminescence quantum efficiencies in DMF solvents were determined by using Coumarin ethanol solution as standard(Φ = 0.56, 1.0 × 10^{-5} mol L^{-1}) on a Perkin–Elmer LS-55B fluorospectrometer by comparison of the fluorescence intensities with that of the compound of known quantum yield under same experimental conditions(shown in Table 1). 1 × 10^{-6} mol L^{-1} compounds HL and Cu(II) complex dilute solutions were prepared in order to avoid possible self-absorption and aggregation. It can been seen from Table 1, upon increasing the solvent polarity, the fluorescence quantum yields exhibit obvious decrease. This behavior accord with previous reports. [24] The quantum yield was calculated according to the following equations: [25]

$$\Phi_S = \Phi_r \left(\frac{A_r(\lambda_r)}{A_s(\lambda_s)} \right) \left(\frac{I(\lambda_r)}{I(\lambda_s)} \right) \left(\frac{{n_s}^2}{{n_r}^2} \right) \frac{\int F_s}{\int F_r} \qquad (2)$$

$$\sigma s = \sigma_r F \Phi_r c_r n_r / F_r \Phi s \, c \, n_s \qquad (3)$$

The two-photon cross section σ was measured by the method reported based on the comparison of fluorescence intensity upon one- and two-photon excitation.[8b,15] From Fig. 3b and Fig. 3c, it can be seen that the 1PEF and 2PEF spectra both located in the same spectral region and have almost identical shapes, which confirm that the emitting states are the same for both processes. Thus, it can be assumed that the fluorescence quantum yield does not change with 1PA or 2PA. The calculated largest T2PA cross-section of the obtained complex in DMF is 1036 GM (1 GM = 10^{-50} cm^4 s $photon^{-1}$) at 760 nm (Fig. 2d), which is about 3 times larger than that of the

corresponding ligand (σ = 374 GM). The experimental result illustrates that the multielectron-donating complex molecular possesses better fluorescence properties at NIR range, which is in agreement with the theoretic result published by Marder [12] and Perry. [13]

3.4 *In vitro* toxicity and tumor cell imaging study

Cytotoxicity is a potential side effect of the compound that must be controlled when dealing with living cells or tissues. In order to this end, cytotoxicity of the prepared complex was investigated against MCF-7 cell lines by the MTT assay (Table 2). As shown in Table 2, for MCF-7 cell line, at low concentration range (10 – 20 μM), the the survival rate of Cu(II) complex is same as propidiumiodide. However, at hight concentration range (40-80 μM), the survival rate of complex slightly highter than that of propidiumiodide. The results suggested that the complex at low-micromolar concentrations did not cause significant reduction in cell viability over a period of 24 h, or even 48 h, and should be safe for further biological studies (more information is shown in Fig. S6). All measurements were performed three times with different wells of plates. The averaged values were presented along with standard deviations.

Table 2 Data of MCF-7 cell survival % (24 h and 48 h)

Compd.	Concen.(μM)	24 h	48 h
HL	10	98.43	96.46
	20	90.17	87.21
	40	80.53	77.52
	80	61.76	58.45
$CuL_2 \cdot C_4H_8O_2$	10	97.62	95.83
	20	87.24	85.68
	40	74.47	73.63
	80	55.32	53.16
propidiumiodide	10	97.53	95.25
	20	86.84	85.37
	40	73.21	70.36
	80	53.21	51.84

As the copper complex has relatively low toxicity toward living cells, fluorescent images of two-photon microscopy of MCF-7 cells labeled with the complex was captured. The human cell lines MCF-7 were cultured and stained with 10 μM of Cu(II) complex. A bright-field (BF) image (Fig. 3a, left) of the cells was obtained immediately prior to the two-photon microscopy imaging. The NIR fluorescence images in vitro indicated that the complex was photoexcited to emit green fluorescence (Fig. 3a, middle), which was clearly observed to locate in the cytoplasm, while a few bright spots in the nucleus.

To distinctly verify their fluorescence stability as fluorescent cellular probes, MCF-7 cells were labeled with both the Cu(II) compound and a nuclear dye propidiumiodide (PI, a commercially available organic dye) simultaneously. The fluorescence of Cu(II) complex and PI in the same cells were monitored under the

same continuous light exposure (480 nm). It can be seen that the Cu(II) complex emitted bright green-colored fluorescence outside the nuclei and the dye PI emitted red-colored fluorescence inside the nuclei from Fig. 3b. We can also find that the green fluorescent signal of the complex was very stable against photobleaching throughout the imaging period of 240 s, while the red fluorescence signal of PI disappeared in 90 s. The results further confirmed the photostability of the obtained complex.

3.5 *In vivo* tumor targeting capability study

It is well-known that the curcumin could effectively be delivered to tumor tissues by Epidermal Growth Factor Receptor(EGFR) effect and taken up by tumor cells as proved in previous papers.[26] As a novel metal complex of curcumin-type, the targeting ability of the Cu(II) complex was investigated with a model of Bel-7402 tumor-bearing mice. In order to quantify the targeting ability of the prepared complex probe, a series of images were collected with the IVIS Lumina imaging system in a dark room at specific time intervals during 10 h after the complex injection. As the blank control group, the images of normal nude mice were also collected at the same time intervals and experimental conditions, which were shown in Figure 3d.

. As shown in Fig. 3c, it can be seen that the live tumor sites were recognizable within 1 h after injection of the probe. As time went on, the probe increasingly accumulated in the live tumor cell and the tumor fluorescence reached the highest intensity at about 5 h after injection. Nevertheless, the tumor fluorescence in the live position began to wear off at about 6 h after injection, and then the fluorescence was

almost completely disappeared from the tumor at about 10 h after injection. The results suggest that the complex is able to target tumor for fluorescent tumor imaging and remains so between 8 and 10 h. Interestingly, the fluorescent intensity from the tumor was found to be significantly stronger than that of corresponding normal mouse, this was mainly due to the higher binding ability of the copper complex (as the monoclonal anti-EGFR antibody, which is the same as the curcumin) to the tumor cells than the noncancerous cells. As many published studies report, most cancerous cells accumulate significantly higher amounts of EGFR during the carcinoma process, and result in different concentration of EGFR on the surface of the cancerous and noncancerous cells.[27]

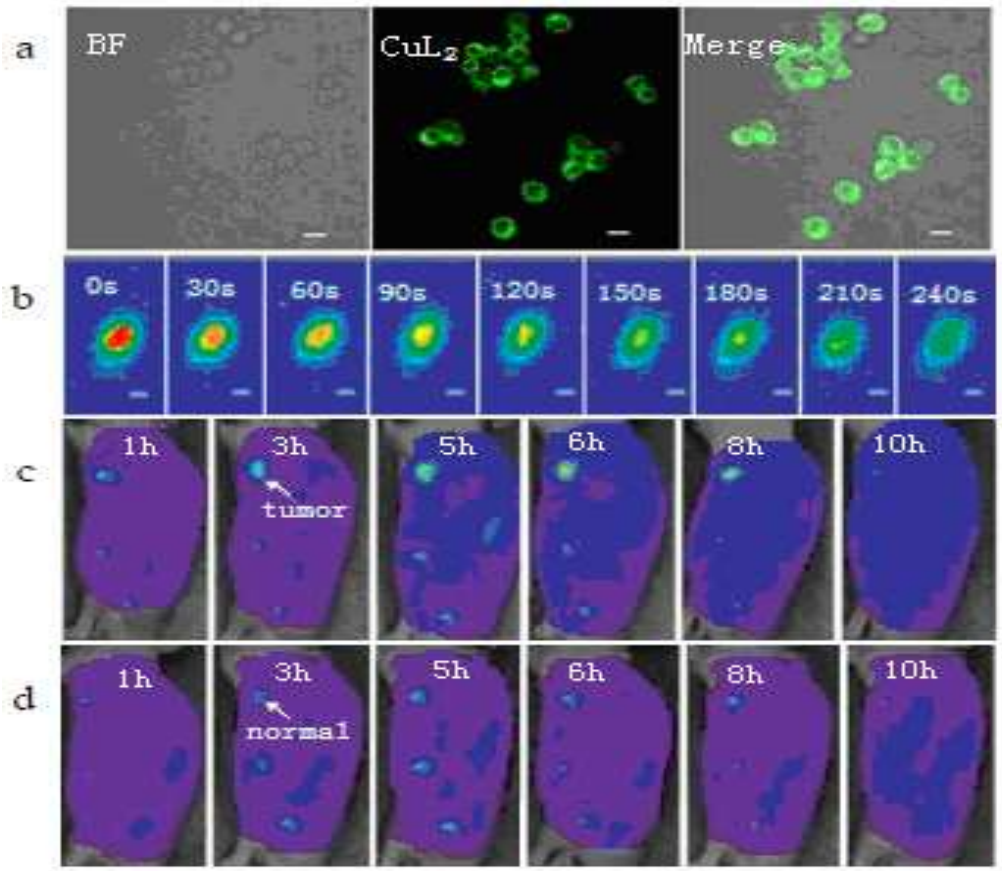

Fig. 3 (a) Cellular uptake and bright-field image of 10 μM CuL_2. (b) The

fluorescent imaging of the MCF-7 cells labeled with the complex (green) and PI (red) at different times under continuous light exposure. (c) The NIR images of Bel-7402 tumor-bearing mice after intravenous injection of the obtained complex. (d) The NIR images of normal nude mice after intravenous injection of the complex. (all the scale bars represent 10 μM).

4. Conclusions

In summary, a novel copper(II) complex containing π-conjugated multibranches has been successfully synthesized and characterized. The Cu(II) complex was investigated both experimentally and theoretically. More intensive 1PEF and 2PEF, and much increased of TPA cross section values σ, were obtained for the moninuclear Cu(II) complex in strong polar media compared to that of the free ligand because of ring system of the complex may favor the ICT and result in an enhanced two-photon absorption. In addition, the NIR fluorescence imaging of the complex *in vivo* was also performed. It was found that the complex can distinguish between cancerous and noncancerous cells, which makes the complex potentially use for cancer diagnoses at the early stage.

Acknowledgements

The authors thank Dr Fucheng Sheng，Hongxing Liu and Ming Zhang from University of Science and Technology of China for valuable technical assistance. This work was financially supported by the National Natural Science Foundation of China (21171001), Department of Education Committee of Anhui Province (KJ2010A222, KJ2010A017), and the Natural Science Foundation of Anhui Province (11040606Q03，1208085MH273).

References

1 (a) D. E. Lee, H. Koo, I. C. Sun, J. H. Ryu, K. Kim and I. C. Kwon, Chem. Soc. Rev., 2012, 41, 2656–2672; (b) G. S. He, L.-S. Tan, Q. Zheng and P. N. Prasad, Chem. Rev., 2008, 108, 1245 – 1330;; (c) Y. He, H. T. Lu, Y. Y. Su, L. M. Sai, M. Hu, C. H. Fan and L. H. Wang, Biomaterials, 2011, 32, 2133-2140; (d) Y. Wang and X. P. Yan, Chem. Commun., 2013, 49, 3324-3326.

2 (a) H..M. Kim, M. S. Seo, M. J. An, J. H. Hong, Y. S. Tian, J. H. Choi, O. Kwon, K. J. Lee and B. R. Cho, Angew. Chem., Int. Ed., 2008, 47, 5167. (b) S. Kim, T. Y. Ohulchanskyy, H. E. Pudavar, R. K. Pandey and P. N. Prasad, J. Am. Chem. Soc., 2007, 129, 2669. (c) Z. Y. Tian and A. D. Q. LI, Accounts of chem. Res., 2013, 46(2),' 269–279.

3 (a) A.M. Lutz, J. K. Willmann, C. W. Drescher, P. Ray, F. V. Cochran, N. Urban, S. S. Gambhir, Radiology, 2011, 259, 329–345. (b) R. Forstner, H. Hricak, K. A. Occhipinti, C. Powell, S. D. Frankel, J. L. Stern, Radiology, 1995, 197, 619-624.

4 C. Fuccio, P. Castellucci, M. C. Marzola, A. Al-Nahhas, S. Fanti, D. Rubello, Clin. Nuc. Med., 2011, 36, 889–893.

5 (a) C. Sun, J. Yang, L. Li, X.Wu, Y. Liu and S. Liu, J. Chromatogr., A, 2004, 803, 173-179; (b) K. Stefflova, J. Chen and G. Zheng, Front. Biosci., 2007, 12, 4709-4716; (c) E. I. Altinoğlu and J. H. Adair, Wiley Interdiscip. Rev.: Nanomed. Nanobiotechnol., 2010, 2, 461- 474.

6 (a) R. M. Williams, W. R. Zipfel, W. W. Webb, Curr. Opin. Chem. Biol., 2001, 5, 603 – 608; (b) W. R. Zipfel, R. M. Williams, W. W. Webb, Nat. Biotechnol. 2003, 21,

1369 –1377; (c) B. G. Wang, K. König, K. J. J. Halbhuber, Microsc. 2010, 238, 1–20.

7 I. H. El-Sayed, X. H. Huang and M. A. El-Sayed, Nano Lett., 2005, 5(5), 829-834.

8 B. Xue, D. W. Deng, J. Cao, F. Liu, X. Li, W. Akers, S.l Achilefub and Y. Q. Gu, Dalton Trans., 2012, 41, 4935–4947.

9 K. Hayashi, M. Nakamura and K. Ishimura, Chem. Commun., 2012, 48, 3830–3832.

10 Z. F. Li, Z. F. Huang, R. Chen, C. Li, S. J. Lin, Y. P. Chen. Chinese J. Lasers, 2009, 36(3), 765-768.

11 (a) Y. H. Jiang, Y. H. Wang, J. L. Hua, J. Tang, B. Li, S. X. Qian and H. Tian, Chem. Commun., **2010**, 46, 4689-4691; (b) S. Kim, Q. D. Zheng, G. S. He, D. J. Bharali, H. E. Pudavar, A. Baev and P. N. Prasad, Adv. Funct. Mater., 2006, 16, 2317-2325.

12 M. Albota, D. Beljonne, L. Brédas, J. E. J. Ehrlich, J. Y. Fu, A. A. Heikal, S. E. Hess, T. Kogej, M. D. Levin, S. R. Marder, D. McCord-Maughon, J. W. Perry, H. Rcckel, M. Rumi, C. Subramaniam, W. W. Webb, X. L. Wu and C. Xu, Science, 1998, 281, 1653-1655.

13 M. Rumi, J. E. Ehrlich, A. A. Heikal, J. W. Perry, S. Barlow, Z. Hu, D. McCord-Maughon, T. C. Parker, H. Rcckel, S. Thayumanavan, S. R. Marder, D. Beljonne, J. L. Bre˙das, J. Am. Chem. Soc., 2000, 122, 9500-9507.

14 (a) G. Began, E. Sudharshan, K. U. Sankar and A. G. A. Rao, J. Agric. Food Chem. 1999, 47, 4992-4998; (b) P. H. Bong, Bull. Korean Chem. Soc., 2000, 21, 81-86.

15 S. S. Zhou, X. Xue, B. Jiang and Y.P. Tian, Science China(Chemistry), 2012, 55(3), 334-340;

(b) S. S. Zhou, X. Xue, J. F. Wang, Y. Dong and Y. Jia, J. Mater. Chem., 2012, 22, 22774-22780; (c) D. M. Li, X. H. Tian, G. J. Hu, Q. Zhang, P. Wang and Y. P. Tian, Inorg. Chem., 2011, 50, 7997-8009.

16 G. M. Sheldrick, SHELXS97 and SHELXS-97. Göttingen: University of Göttingen; 1997.

17 (a) G. Y. Xu, D. Wei, J. F. Wang, S. S. Zhou, B. L. Wu, M. H. Jiang, Dyes and Pigments, 2014, 101, 312-317; (b) J. K. Clegg, L. F. Lindoy, J. C. McMurtriea and D. Schiltera, Dalton Trans, 2005, 857-863.

18 H. Takakura, M. Hattori, M. Takeuchi, and T. Ozawa, ACS Chem. Biol. 2012, 7, 901 910.

19 T. Shiga, M. Ohba and H. Ohkawa, Inorg. Chem., 2004, 43, 4435-4462;

20 (a) L. Li, Y. P. Tian, J. Y. Yang, P. P. Sun, J. Y. Wu, H. P. Zhou, S. Y. Zhang and M. H. Jiang, Chem. Asian J., 2009, 4, 668-675; (b) Q. D. Zheng, G. S. He and P. N. Prasad, J. Mater. Chem., 2005, 15, 579-586.

21 (a) Y. P. Xie, X. F. Zhang, Y. Xiao, Y. D. Zhang, F. Zhou and J. L. Qu, Chem. Commun., 2012, 48, 4338-4340; (b) Y. X. Yan, X. T. Tao, Y. H. Sun, C. K. Wang, G. B. Xu and M. H. Jiang, J . Mater. Chem., 2004, 14, 2995-3003; (c) M. H. V. Werts, S. Gmouh, O. Mongin, T. Pons and B. D. Mireille, J. Am. Chem. Soc., 2004, 126, 16294-16299.

22 J. R. Lakowicz, Plenum Press, New York, **1983**, p. 190.

23 (a) Y. Ren, X. Q. Yu, D. J. Zhang, D. Wang, M. L. Zhang, G. B. Xu, Y. P. Tian, Z. S. Shao and M. H. Jiang, J. Mater. Chem., 2002, 12, 3431-3438; (b) Y. Ren, Q. Fang, W. T. Yu, Y. P. Tian and M. H. Jiang, J. Mater. Chem., 2000, 10, 2025-2030.

24 (a) J. E. Rogers, J. E. Slagle, D. G. McLean, R. L. Sutherland, B. Sankaran and P. A. Fleitz, J. Phys. Chem. A, 2004, 108, 5514-5519; (b) D. X. Cao, Q. Fang, D. Wamg, Z. Q. Liu, G. Xue and G. B. Xu, Eur. J. Org. Chem., 2003, 3628-3633; (c) L. M. Fu, X. F. Wen, X. C. Ai, Y. Sun and J. P. Zhang, Angew. Chem., 2005, 117, 757-762.

25 (a) S. S. Zhou, Q. Zhang, X. H. Tian, G. J. Hua, F. Y. Hao, J. Y. Wu and Y. P. Tian, Dyes and Pigm., 2011, 92, 689-696; (b) H. P. Zhou, D. M. Li , J. Z. Zhang, J. Y. Wu, Y. P. Tian and M. H. Jiang, Chem. Physics, 2006, 322, 459-465.

26 (a) H. Aoki, Y. Takada, S. Kondo, R. Sawaya and B. B. Aggarwal, Mol. Pharmacol., 2007, 72, 29-35; (b) B.B. Aggarwal, S. Banerjee, U. Bharadwaj, B. Sung, and S. Shishodia, Biochem. Pharmacol., 2007, 73(7), 1024-1030; (c) S. Lev-Ari, A. Starr, A. Vexler, V. Karaush, V. Loew, J. Greif, E. Fenig and D. Aderka, Anticancer Res., 2006, 26(6B)：4423-4434; (d) A. Chen, J. A. Xu, J. Physiol. Gastrointest Liver Physiol., **2005**, 288(3), 447-452.

27 (a) R. Rosell, Y. Ichinose, M. Taron, C. Sarries, C. Queralt, P. Mendez, J. M. Sanchez, K. Nishiyama and T. Moran, Lung Cancer, 2005, 50, 25-30; (b) W. Pao, V. A. Miller, J Clin Oncol, 2005, 23, 2556-2561; (c) I. H. El-Sayed, X. H. Huang and M. A. El Sayed, Nano Lett., 2005, 5(5), 829-831.

A table of contents entry.

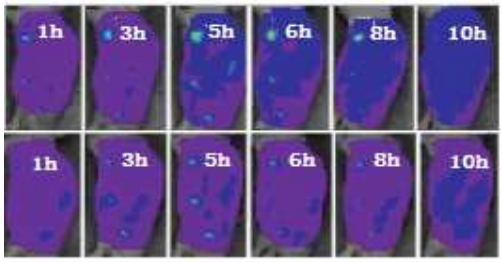

The results of TPEF imaging in tumor-bearing mouse model demonstrated the potential of obtained complex for *in vivo* tumor diagnosis.